Improvement of the Diffusive Component of Dark Current in Silicon Photomultiplier Pixels

Roberto Pagano, Sebania Libertino, Domenico Corso, and Salvatore Lombardo
Istituto per la Microelettronica e Microsistemi,
Consiglio Nazionale delle Ricerche (CNR)
VIII Strada Z.I. 5, 95121, Catania, Italy
roberto.pagano@imm.cnr,it,
sebania.libertino@imm.cnr.it,
domenico.corso@imm.cnr.it,
salvatore.lombardo@imm.cnr.it

Giuseppina Valvo, Delfo Sanfilippo, Giovanni Condorelli, Massimo Mazzillo, Angelo Piana, Beatrice Carbone, and Giorgio Fallica
IMS-R&D
STMicroelectronics
Stradale Primosole, 50 95121 Catania, Italy
giusy.valvo@st.com, delfo.sanfilippo@st.com,
giovanni.condorelli@st.com,
massimo.mazzillo@st.com, angelo.piana@st.com,
beatrice.carbone@st.com, giorgio.fallica@st.com.

***Abstract*— The temperature behavior of dark current in SiPM pixels was studied for two fabrication technologies differing in the anode contact. The first (old) technology had the contact on the front, while the second (new) has the anode contact on the back. The layout changes allowed us to obtain a strong reduction of the dark current diffusive component thus strongly improving the device performances.**

Keywords-Silicon Photomultipliers (SiPM); Dark Counts.

I. INTRODUCTION

Silicon Photomultipliers (SiPMs) are a very promising technology to complement or even replace conventional vacuum tube photomultipliers, given their strong advantages in terms of cost, mechanical robustness, reliability, and insensitivity to magnetic field [1-4]. These devices are the parallel connection of pixels, each one consisting in a p-n junction suitably doped in order to have avalanche breakdown in a well defined active area with a quenching resistance in series. The active area is formed by creating an enriched well, generally doped by ion implantation followed by thermal processing for dopant activation and defect annealing. This dopant local enrichment generates regions where the vertical junction electric field is higher, and these become the device active areas for photon detection [5]. The p-n junction devices are operated in Geiger mode [6], that is, they are biased above the junction breakdown voltage (BV). The single pixel operation is as follows: when the device is quiescent its active area is characterized by an electric field well above the breakdown field. In such a condition the absorption of a single photon in the active area will trigger, through the generation of an electron-hole pair, with a nearly 100% probability, the onset of the junction avalanche. The voltage drop across the series resistance, which decreases the voltage applied to the p-n junction, quickly quenches the avalanche. Therefore the photon arrival results in a current pulse which can then be easily measured by an external circuit. The avalanche quenching, moreover, restores the pixel to the original condition of electric field above BV, rendering the pixel ready to the detection of a new photon [6]. The operation of the overall SiPM is simply the sum of the behaviors of the various pixels. Therefore, this device compared to the original design of the Single-Photon Avalanche Diode (SPAD) has the advantage of having a relatively large dynamic range response proportional to the flux of photons impinging on the detector at the same time [7].

The SiPM major drawback is the relatively large dark current, due to the combination of a diffusion current produced at the quasi-neutral regions at the boundaries of the device active region, and of generation of carriers due to point defects and/or metallic impurities in the active area depletion layer emitting carriers through the Schockley-Hall-Read (SHR) mechanisms, eventually boosted by the Poole-Frenkel effect [8].

In previous works [9-12], we investigated the dark current of SiPM devices produced by STMicroelectronics. After the first two work [9-10] that was essential to comprehend that that the single pixel dark current in the first developed SiPM technology is due to the above two mentioned processes and that have different weight varying the temperature, we finally understood [12] that the first process, the diffusion of minority carriers, is relevant for temperatures below 10 °C and it is primary localized at the lateral border of the pixel, while the latter, the carriers generation through SHR mechanism, dominates at higher temperatures and is localized in the active area of the pixel. Hence, at 25 °C, the dark current is limited by the lateral diffusion of minority carriers. This is an intrinsic effect, due to the diffusion of minority carriers towards the p-n junction depletion layer, inversely proportional to the doping level and, therefore, larger at the perimeter of the active area, where the dopant concentration is lower. Being an intrinsic effect, one may conclude that the dark current levels of the above mentioned SiPM devices, at least at 25 °C, are the ultimate limit, which cannot be subjected to further improvements. In principle, however, this is not true, since

 ISBN: 978-1-61208-208-0

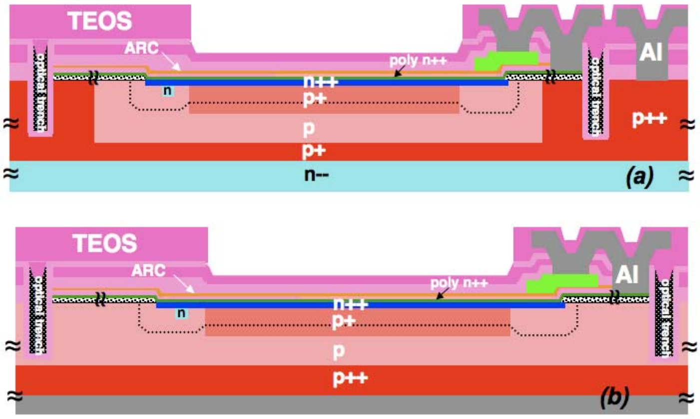

Figure 1. Schematic cross-section of a SiPM pixel (not in scale). (a) Old technology with double epitaxial layer, n-substrate and trenches crossing the sinker diffusion. (b) New technology with single epitaxial layer, p-substrate, and isolated sinker diffusion. Dotted black lines remark the depleted region extension.

the diffusion currents that leads to the dark current is expected to be also inversely proportional to the square root of minority carrier lifetime. Any strong improvement in the minority carrier lifetime would therefore translate into a dark current improvement.

In this paper, we show that a new device architecture, investigated in [11], does provide such a strong lifetime and the dark current improvement.

II. EXPERIMENTAL

The full device fabrication details can be found in [13]. In this paper, we want to focus our attention on similarities and differences between the two technologies in study. They have the same active part and guard ring of the device, fabricated and discussed in [9-13], thus producing the same BV (-28V at 25°C). The main difference between the two technologies is in the substrate: in the first technology a double epitaxial layer, first p^+, then followed by a p^- is grown on a low doped n-type (100) oriented Si substrate [9,10,12]. In the second technology [11,13], only a single p^- epitaxial layer is grown on a highly doped p^+ (100) Si substrate. In both cases deep optical trenches are realized for the optical and electrical isolation between the pixels. Figure 1 shows the schematic cross section of the device, not in scale, for the two technologies, old and new (Fig. 1a and b, respectively). A further difference in the two devices is that in the new technology is not needed the presence of the anode contact on the front, hence the p^+ region between the active area and the optical trench has been removed (see Fig. 1).

Electrical characterization was performed at wafer level using a Cascade Microtech Probe Station *11000*. The samples were cooled using a Temptronic *TPO 3200A* ThermoChuck that provide a stabilized temperature between -60°C and 200°C. Current vs. voltage measurements (I-V) were acquired using an *HP 4156B* precision semiconductor parameter analyzer using an integration time of 1s. The dark count was obtained using a Tektronix *DPO 7104* Digital Oscilloscope with 1 GHz bandwidth and 20 Gsa/s. The I-V characteristics have been measured on more than 30 SiPM pixels of old and new technologies, showing a very good uniformity.

III. RESULTS AND DISCUSSIONS

Dark currents of single SiPM pixels fabricated in the two different technologies were investigated with respect to voltage and temperature (from -25°C to 65°C). Figure 2 shows the dark currents as a function of voltage at three different temperatures, -25°C (circles), 25°C (triangles) and 65°C (squares) of a SiPM pixel fabricated in the old technology (filled symbols) compared to the dark current of a pixel in the new technology (open symbols). At -25°C the dark currents (circles) are of the same order of magnitude, while by increasing the temperature they show remarkable differences. At 25°C and at V_{BIAS} = -32V (+ 4V overvoltage, OV) the dark current in the old technology is one order of magnitude higher than that of the new technology one. At 65°C the difference increases (two orders of magnitude of difference).

In order to understand the reason of such reduction, we extracted the activation energy of the dark current for the two devices as a function of the temperature. The Arrhenius plot of the dark current for a constant OV (+4V in Fig. 3) evidences a clear reduction of the diffusion component in the new technology. In particular, at low temperatures the dark current is dominated by SHR generation from mid-gap level defects of similar density in both technologies, as demonstrated by the measured activation energies, reported

TABLE I. MEASURED VALUE OF THE DC AT 25°C; ACTIVATION ENERGIES EXTRACTED FROM THE ARRHENIUS PLOT OF FIGURE 3; SOME OF THE PARAMETERS USED IN THE DC SIMULATION.

Technology	DC (s-1)	E_{A1} (eV)	E_{A2} (eV)	N_{DEF} (cm^{-3})	E_C-E_T (eV)	τ_n (s)
Old	600	0.57	1.18	10^{-9}	0.55eV	10×10^{-6}
New	4600	0.59	1.12	10^{-9}	0.55eV	3×10^{-3}

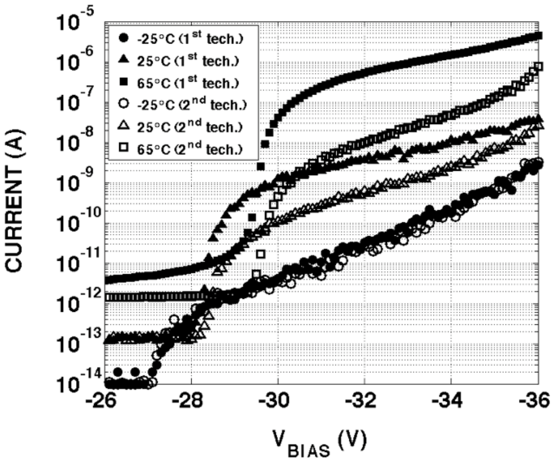

Figure 2. Dark currents at three different temperatures, -25°C (circles), 25°C (triangles) and 65°C (squares) of SiPM pixels fabricated in the old technology (filled symbols) and new technology (open symbols).

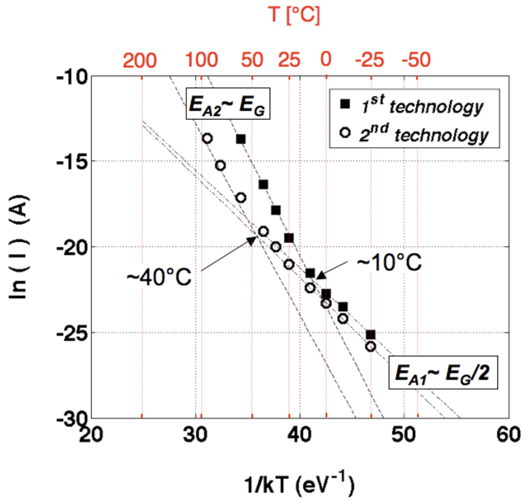

Figure 3. Arrhenius plot of the dark currents at constant +4 V overvoltage for a SiPM pixel fabricated in the old technology (filled squares) and in the new (open circles) technology.

in Table I. At higher temperatures, the diffusion of minority carriers becomes the dominant mechanism of dark current. Note, however, that this mechanism becomes the leading effect at different temperatures for the two technologies. For the old one the diffusion mechanism dominates for temperatures above 10°C, while for the second one it prevails at temperatures above 40°C.

To get a further insight, the dark count (*DC*) rates for the two devices were measured as a function of temperature and bias voltage (Fig. 4). In general, it has been demonstrated that the DC rate in a pixel is well described by the following equation [10,12]:

$$DC = DC_{SHR} + DC_{DIFF} \tag{1}$$

The first term, DC_{SHR}, takes into account the SHR generation from mid-gap level defects located in the depleted active volume of the pixel p-n junction:

$$DC_{SHR} = N_{Def} \cdot A_{ACT} \cdot W \cdot \gamma_n \cdot \sigma_n \cdot T^2 \cdot \exp\left(-\frac{E_C - E_T}{kT}\right) \tag{2}$$

where N_{Def} is the defect concentration, W the depletion layer width, A_{ACT} the pixel active area, γ_n the universal constant for emissivity [14], σ_n the defect cross-section, E_C-E_T the defect ionization energy [14], T the temperature, and k the Boltzmann constant.

The second term DC_{DIFF} is the component due to the minority carrier diffusion from the perimeter of the pixel active area into the active depleted volume, given by:

$$DC_{DIFF} = A_P \cdot \sqrt{\frac{D_n}{\tau_n}} \cdot \frac{n_i^2}{N_a} \tag{3}$$

where n_i is intrinsic carrier concentration, N_a is the dopant concentration of the epitaxial layer in the active area perimeter, D_n is the electron diffusivity, τ_n is the minority carrier lifetime and A_P the area of the perimeter zone surrounding the active area.

Figure 4 shows the comparison of the experimental (symbols) and the simulated DC rates (continuous and dashed line) using Eqs. (1), (2) and (3) for the old and the new technology respectively at different temperatures. The agreement between data and simulation is extremely good in the full temperature range explored. We modeled the experimental data by assuming $N_{Def} = 10^9$ cm^{-3}, E_C-$E_T = 0.55$ eV, $\sigma_n = 1.6\times10^{-15}$ cm^2, with the universal constant $\gamma_n = 1.78\times10^{21}$ cm^{-2} s^{-2} K^{-2} for the SHR term (Eq. (2)) in both technologies. For the diffusion term (Eq. (3)) we assumed: μ_n=1500 cm^2/Vs and N_a= 10^{15} cm^{-3}, that is the dopant concentration of the p- epitaxial layer. To explain the large difference in the DC rate in the diffusion regime, we have to assume drastically different values of minority carrier lifetime: τ_n = 10 μs for the old technology and τ_n = 3 ms for the new technology. The large lifetime improvement results in a noticeable improvement of the *DC* rate diffusive component, as shown in Figs. 3 and 4. The reason for such radical improvement of both lifetime and *DC* rate in the diffusive regime may be ascribed to the different device architecture (see Fig. 1). In the old technology a large p-type dopant concentration in the device periphery, up to a B concentration of the order of 2×10^{18}/cm^3, is present, while it is completely absent in the new technology. By considering that the Auger effect [15-16] for such a large dopant concentration becomes a relevant recombination mechanism, with lifetimes of the order of 1 μs in correspondence with the peak B concentrations at the periphery, we propose that the low effective minority carrier lifetimes observed in the old technology are due to Auger recombination occurring at the device periphery. Such effect disappears in the new technology, resulting in a noticeable improvement of lifetime and, therefore, of *DC* rate in the diffusive regime. In the present new generation technology, the defect concentration is of the order of $10^9/cm^3$, hence the diffusive component dominates the *DC* rate at about 50°C and above. By further decreasing the concentration of SHR defects, the *DC* rate would be limited only by the diffusive regime also at room temperature (25 °C), which would result in a level of *DC* rate of a few tens of counts per second for our pixel size.

IV. CONCLUSIONS

In this paper, we have reported on the comparison of two SiPM pixel architectures: the first one has a double epitaxial layer p+/p on an n-type Si substrate and the anode contact is on the top of the structure; the second one has only a single p^- epitaxial layer grown on a highly doped p^+ Si substrate with the anode contact at the bottom of the structure. In both cases deep optical trenches are realized.

The dark current behavior of SiPM pixels with respect to the temperature was studied for the two fabrication technologies. The realization of a back-side anode contact results in a major improvement of the minority carrier lifetime, probably due to the reduction and/or removal of Auger recombination at the device periphery taking place when a high B doping is used to provide the front side anode contact. This results in a noticeable improvement of the diffusive component of the *DC* rate and then to a reduction of the pixel *DC* for temperature higher than 10°C.

ACKNOWLEDGMENT

This work was partially supported by STMicroelectronics under Grant CDR.ST.CNR-IMM.MATIS.24.02.2010.002

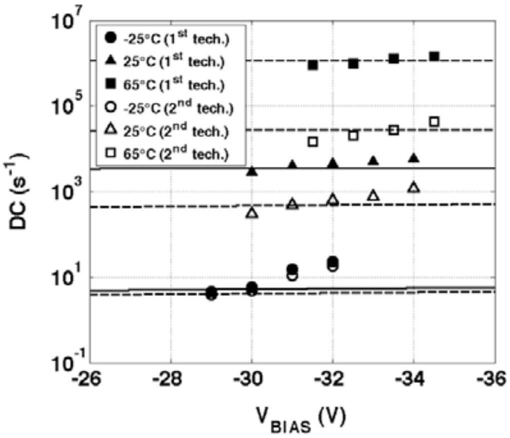

Figure 4. Comparison of DC at three different temperatures, -25°C (circles), 25°C (triangles) and 65°C (squares) of the two SiPM pixels fabricated in the old (filled symbols) and new (opens symbols) technologies. Continuous and dashed lines are the simulated DC as described in text for the old and the new technology respectively.

REFERENCES

[1] N. Otte, B. Dolgoshein, J. Hose, S. Kleminin, E. Lorentz, R. Mirzoyan, E. Popova, and M. Teshina, “The Potential of SiPM as Photon Detector in Astroparticle Physics Experiments like MAGIC and EUSO”, Nucl. Instr. and Meth. in Phys. B Proc. Suppl., vol. 150, 2006, pp. 144-149.

[2] V. D. Kovaltchouk, G. J. Lolos, Z. Papandreou, and K. Wolbaum, “Comparison of a silicon photomultiplier to a traditional vacuum photomultiplier”, Nucl. Instr. and Meth. in Phys. A, vol. 538, 2005, pp. 408-415.

[3] P. Finocchiaro, A. Pappalardo, L. Cosentino, M. Belluso, S, Billotta, G. Bonanno, and S. Di Mauro, “Features of Silicon Photo Multipliers: Precision Measurements of Noise, Cross-Talk, Afterpusing, Detection Efficiency, IEEE Trans. Nucl. Sci., vol. 56, 2009, 1033-1041.

[4] A. Del Guerra, N. Belcari, M. G. Bisogni, G. LLosa, S. Marcatili, G. Ambrosi, F. Corsi, C. Marzocca, G. Dalla Betta, and C. Piemonte “Advantage and pitfalls of the silicon photomultiplier (SiPM) as photodetector for the next generetaion of PET scanners”, Nucl. Instr. and Meth. in Phys. A, vol. 617, 2010, pp. 223-226.

[5] E. Sciacca, A. C. Giudice, D. Sanfilippo, F. Zappa, S. Lombardo, R. Consentino, C. Di Franco, M. Ghioni, G. Fallica, G. Bonanno, S. Cova, and E. Rimini, “Silicon Planar Technology for Single-Photon Optical Detectors” IEEE Trans. Elec. Dev., vol. 50, 2003, pp. 918-925.

[6] S. Cova, M. Ghioni, A. Lacaita, C. Samori, and F. Zappa, “Avalanche photodiodes and quenching circuits for single-photon detection”, Appl. Opt., vol 35, 1996, pp. 1956-1976.

[7] D. Renker and E. Lorentz, “Advances in solid state photon detectors” J. Instrum., vol. 4, 2009, p.04004.

[8] S. Cova, A. Lacaita, and G. Ripamonti, “Trapping Phenomena in Avalanche Photodiodes on Nanosecond Scale” IEEE Electron Dev. Lett., vol. 12, 1991, pp. 685-687.

[9] R. Pagano, S. Libertino, G. Valvo, G. Condorelli, B. Carbone, A. Piana, M. Mazzillo, D. N. Sanfilippo, G.G. Fallica, G. Falci, and S. Lombardo, “Dark Count in Single Photon Avalanche Si Detectors”, Proc. Of SPIE, vol. 7598, 2010, p. 75980Z-1-8.

[10] R. Pagano, S. Lombardo, S. Libertino, G.Valvo, G. Condorelli, B. Carbone, D. N. Sanfilippo, and G. Fallica, “Understanding dark current in pixels of silicon photomultipliers, proc. IEEE European Solid-State Device Research Conference, (ESSDERC 2010), IEEE press, Sept. 2010, pp. 265-268.

[11] R. Pagano, D. Corso, S. Lombardo, S. Libertino, G. Valvo, D. Sanfilippo, A. Russo, P. G. Fallica, A. Pappalardo, and P. Finocchiaro, “Optimized silicon photomultipliers with optical trenches”, proc. IEEE European Solid-State Device Research Conference, (ESSDERC 2011), IEEE press, Sept. 2011, pp. 183-186.

[12] R. Pagano, D. Corso, S. Lombardo, G. Valvo, D.N. Sanfilippo, G. Fallica, and S. Libertino, “Dark current in SiPM pixel: data and model”, IEEE Trans. Electron Dev. (in press).

[13] M. Mazzillo, G. Condorelli, D. Sanfilippo, G. Valvo, B. Carbone, G. Fallica, S. Billotta, M. Belluso, G. Bonanno, L. Cosentino, A. Pappalardo, and P. Finocchiaro, “Silicon Photomultiplier Technology st STMicroelectronics”, IEEE Trans. Nucl. Sci., vol. 56, 2009, pp. 2434-2442.

[14] D. K. Schroder, *Semiconductor Material and Device Characterization 3rd ed.*, Wiley-Interscience, 2006, pp. 262-264.

[15] L. Passari and E. Susi, “Recombination mechanisms and doping density in silicon”, J. Appl. Phys., vol. 54, 1983, pp 3935-3937.

[16] D. K. Schroder, “Carrier Lifetimes in Silicon”, IEEE Trans. Electron Dev., vol. 44, 1997, pp. 160-170.